A COMPARISON OF NUMERICALLY DETERMINED DIVERGENT AND NON-DIVERGENT WINDS TO GEOSTROPHIC WINDS

FRED ERNST LACEY

A COMPARISON OF NUMERICALLY DETERMINED DIVERGENT AND NON-DIVERGENT WINDS TO GEOSTROPHIC WINDS

* * * * *

Fred Ernst Lacey

A COMPARISON OF NUMERICALLY DETERMINED DIVERGENT AND NON-DIVERGENT WINDS TO GEOSTROPHIC WINDS

by

Fred Ernst Lacey

Captain, United States Marine Corps

Submitted in partial fulfillment of
the requirements for the degree of

MASTER OF SCIENCE
IN
METEOROLOGY

United States Naval Postgraduate School
Monterey, California

1964

A COMPARISON OF NUMERICALLY DETERMINED DIVERGENT AND NON-DIVERGENT WINDS TO GEOSTROPHIC WINDS

by

Fred Ernst Lacey

This work is accepted as fulfilling

the thesis requirements for the degree of

MASTER OF SCIENCE

IN

METEOROLOGY

from the

United States Naval Postgraduate School

ABSTRACT

Numerical weather analysis relies heavily on numerically computed winds both for direct output and internally for calculating advection and other purposes. It is the intent of this paper to compute, analyze, and compare the geostrophic, the non-divergent, the divergent, and a combination of the latter two. Where there occurs a significant difference between these numerically derived winds, an attempt is made to compare each to the observed winds. This study is made for all standard levels through 300 mb. Data and several computer programs were furnished by the U. S. Navy Fleet Numerical Weather Facility, Monterey, California.

The writer wishes to express his appreciation to Professor George J. Haltiner of the U. S. Naval Postgraduate School for his guidance, contributions and encouragement in this work.

Appreciation is expressed to Lieutenant Commander Mildred J. Seljos, United States Navy for aid and advice in programming. Further thanks are extended to Lt. R. F. Alden, U. S. Navy, and Lt. G. C. Rosenberger who provided programs for computation of horizontal velocity divergence and for advection of temperature.

TABLE OF CONTENTS

Table of Symbols

g	the upward component of the apparent gravitational acceleration
D	the altimeter correction $D = Z - Z_p$
Z_p	the height of an isobaric surface
Z	the pressure altitude in the standard atmosphere
f	the Coriolis parameter, $2\ \Omega \sin\phi$, where ϕ is the geographical latitude
$\bar{f}$	the mean value of the Coriolis parameter, $2\ \Omega \sin 45^\circ$
Φ	the geopotential
ζ	the relative vorticity $\zeta = \frac{\partial v}{\partial x} - \frac{\partial u}{\partial y}$
η	the absolute vorticity $\eta = \zeta + f$
Ψ	the stream function for the non-divergent component of velocity
χ	the velocity potential for the divergent component of velocity
ω	the vertical velocity of air in pressure coordinates
P	the atmospheric pressure in millibars
σ	the static stability $\sigma = -\frac{T}{\Theta}\frac{\partial \Theta}{\partial p}$
R	the universal gas constant
d	grid distance, 381 km at 60N
m	map scale factor
∇	del operator on a constant-pressure surface
∇^2	horizontal Laplacian operator on a constant-pressure surface
J	horizontal Jacobian operator $J(A,B) = \frac{\partial A}{\partial x}\frac{\partial B}{\partial y} - \frac{\partial A}{\partial y}\frac{\partial B}{\partial x}$

∇^2	finite difference Laplacian $\nabla^2 A = (A^{j}_{i+1} + A^{j+1}_{i} + A^{j}_{i-1} + A^{j-1}_{i} - 4A^{j}_{i})$
$\mathbb{J}$	finite differnece Jacobian $\mathbb{J}(A,B) = \left[(A^{j}_{i+1} - A^{j}_{i-1})(B^{j+1}_{i} - B^{j-1}_{i}) - (A^{j+1}_{i} - A^{j-1}_{i})(B^{j}_{i+1} - B^{j}_{i-1})\right]$
Vg	geostrophic wind
Ve	non-divergent wind
$V\Psi$	Ve
Vx	divergent wind
Vt	total wind
Va	actual wind as measured from soundings
¢	dummy variable
I¢	wind speed of V¢
DGD¢	difference in wind direction, Dg - D¢
IGI¢	difference in wind speed, Ig - I¢
DADV	advection of absolute geostrophic vorticity by Vg
EADV	advection of absolute stream function vorticity by Ve
TADV	advection of absolute stream function vorticity by Vt
XADVT	advection of temperature with Vx
t	time
u¢	u component of V¢
v¢	v component of V¢
D¢	wind direction of V¢

1. Introduction

One of the primary products of any numerical weather facility is wind data for operational use and for further numerical computations such as advection. It is the purpose of this paper to analyze and compare several types of numerically derived winds. The types considered are the geostrophic, Vg, the non-divergent, Ve, the divergent, Vx, and finally the total wind, Vt, which is a combination of the divergent and non-divergent parts of the wind. These winds are calculated by solution of appropriate equations using data from the U.S. Naval Fleet Numerical Weather Facility, Monterey, California (FNWF). Computations were made on the U. S. Naval Postgraduate School CDC 1604 digital computer.

Comparison of these winds is made at all standard levels through the 300-mb level by calculation of speed and geographical direction on separate maps for each level covering the Northern Hemisphere. Difference fields of direction and speed are made between each wind and the geostrophic wind. Vertical cross sections were computed and studied for each of the winds and for the difference fields. Further comparisons and analyses are made by using these three winds to advect absolute vorticity. Advection of temperature was also computed using Vx.

2. Background

The geostrophic wind is computed from the well known formula

$$\mathbb{V}_g = -\frac{g}{f}\left(\frac{\partial D}{\partial y}\hat{i} - \frac{\partial D}{\partial x}\hat{j}\right) \qquad (1)$$

utilizing a standard program of FNWF. This program generates fields of geostrophic wind directions in degrees and speed in knots. All computations were done on the FNWF square grid centered on the North Pole and consisting of 3968 with a grid interval of 381 km at 60N. In this program the sine of latitude, as required in computation of the coriolis parameter, f, was set equal sine 15 degrees. The latter points were not utilized in the evaluation of results.

Geostrophic wind, Vg, is utilized as a basis of comparison for later derived non-divergent, Ve, and total, Vt, winds.

The Helmholtz theorem allows expression of the wind as the sum of the divergent and non-divergent components.

$$\mathbb{V} = \hat{k} \times \nabla \psi + \nabla \chi. \qquad (2)$$

Winds of this form will be hereafter referred to as total wind, Vt.

The potential function χ for the divergent part of the wind is obtained through relaxation of the Poisson-type continuity equation

$$\nabla^2 \chi + \frac{\partial \omega}{\partial p} = 0. \qquad (3)$$

The stream function, Ψ, for the non-divergent portion of the wind is approximated by solution of the balance equation

$$\nabla^2 \psi + \nabla \psi \cdot \nabla f - \frac{2}{f}\left[\left(\frac{\partial^2 \psi}{\partial x \partial y}\right)^2 - \frac{\partial^2 \psi}{\partial x^2}\frac{\partial^2 \psi}{\partial y^2}\right] = \frac{1}{f}\nabla^2 \Phi \qquad (4)$$

Here, Φ is the geopotential.

The vertical component of vorticity, ζ, is the Laplacian of the stream function

$$\zeta = \nabla^2 \psi \qquad (5)$$

and absolute vorticity, η, is the sum of ζ and the vertical component of the earths vorticity, f,

$$\eta = \zeta + f. \qquad (6)$$

Vertical velocity, ω, is computed by the diagnostic equation

$$\nabla^2(\sigma\omega) + \frac{Pf\eta}{R}\frac{\partial^2 \omega}{\partial P^2} = \frac{g}{f}\left[\nabla^2 J(D,T) - J(D,\nabla^2 T) - \frac{f}{g} J(T,\eta)\right] \qquad (7)$$

developed by Haltiner, Clarke, and Lawniczak [1].

For convenience the stream function has been redefined so as to be in units of height,

$$\psi = \frac{g}{f} E. \qquad (8)$$

The geostrophic advection of absolute geostrophic vorticity is computed from the expression

$$-\frac{g}{f} J(D, \eta_g) \qquad (9)$$

and the advection of η_e by

$$-\frac{g}{\bar{f}} J(E, \eta_e). \tag{10}$$

The advection of η_e by Vx is computed from the formula

$$V_x \cdot \nabla \eta_e = u_x \frac{\partial \eta_e}{\partial x} + v_x \frac{\partial \eta_e}{\partial y} . \tag{11}$$

(10) and (11) are combined to represent advection of η_e by Vt and compared to similar advection using Vg and Ve.

3. Procedures

The sequence of calculations programmed started with solution of the geostrophic wind equation in finite difference form

$$V = -\frac{gm}{2fd}\left[(D_i^{j+1} - D_i^{j-1})\hat{i} - (D_{i+1}^{j} - D_{i-1}^{j})\hat{j}\right] \quad . \tag{12}$$

Fields of u_g and v_g relative to map projection were generated and converted into fields of wind direction in geographical headings at each grid point. Likewise, fields of isotachs were produced and printed in contoured map form. These calculations and maps were made for all standard levels to 300 mb for this and all subsequent programs.

The balance equation, (4), as programmed by M. Reese of FNWF, was then solved and the fields of E values were stored on magnetic tape. The iterative scheme of this program does not always converge at 300 mb or has an excessive running time, both of which limited the data produced. The E values were then used as input to the geostrophic wind program with the appropriate substitution of f for $\bar{f}$. These "balanced" winds were computed and stored in the same manner as Vg.

Divergence fields are taken as input for solution of (3). Here, as with Ψ, χ is redefined as

$$\chi = \frac{g}{\bar{f}}\hat{\chi} \tag{13}$$

so that the velocity potential has units of height and therefore is compatable with E and D for use in (12) with minor changes. Expressing the first term of equation (3) in finite difference form gives

$$\nabla^2 \hat{\chi} = -\frac{\bar{f}}{g}\frac{d^2}{m^2}\frac{\partial \omega}{\partial p} \tag{14}$$

which may be solved by use of an FNWF Poisson relaxation program. The derivitive $-\partial \omega / \partial p$ which is the horizontal divergence of the wind is evaluated by a finite difference approximation as programmed by Alden and Rosenberger [2] .

The χ fields are then used to compute the divergent wind component by the finite difference equation

$$V_\chi = \frac{gm}{2\bar{f}}\left[(\hat{\chi}^{j}_{i+1} - \hat{\chi}^{j}_{i-1})\hat{i} + (\hat{\chi}^{j+1}_{i} - \hat{\chi}^{j-1}_{i})\hat{j}\right] \tag{15}$$

Again the u and v components are stored and maps of direction and of isotachs are produced.

Now the components of Ve and Vx are added and a field of these combined components produced as follows

$$u_\Psi + u_\chi = u_t \tag{16.a}$$

$$v_\Psi + v_\chi = v_t \tag{16.b}$$

As before these component fields are stored and maps of each level printed.

Programs to aid comparison and analysis are now written. Analysis of directional differences is made by using the direction fields of Vg as a basis and subtracting directions of Ve and Vt from it. This proved to

be a challenging problem for several reasons. First, directions are by nature discontinuous at singular points on isogons maps and also in general at 360 degrees. Second, direction tends to vary widely in the vicinity of small scale features that are not concentric between the various fields compared.

The discontinuity problem was solved successfully with a rather intricate program. However, the singular points and non-concentric small scale features still caused a large gradient of direction and difficult contouring to plot or read. This problem was alleviated by replacing a value of minus zero at all points on the directional difference maps at which the wind speed was less than five knots. This improved appearance of the maps and facilitated evaluation. Moreover the minus zero values still indicated those areas where singular points had occurred. The 5-knot criterion proved to be of no detriment in subsequent use.

Speed-difference fields, IGIE and IGIT, are produced by the same program as directional difference. The computation of speed differences included a statistical analysis and grid maps of output included the pillow, P, and root-mean-square difference, RMSD. These terms are defined in APPENDIX I.

Another series of programs were written to calculate the advection of absolute vorticity, η , by the various winds previously computed and to compare the results.

First, fields of D values are used as input to evaluate the geostrophic vorticity

$$\eta_g = \frac{g m^2}{d^2 f} \nabla^2 D + f \tag{17}$$

with an FNWF program. Then the resulting fields from (17) are used to obtain

$$\Delta_t \zeta = -\frac{g \Delta t m^2}{4 d^2 f} JJ(D, \eta_g) \tag{18}$$

which is plotted on standard grid maps. This program is then internally modified to solve

$$\eta_e = \frac{g m^2}{d^2 \bar{f}} \nabla^2 E + f \tag{19}$$

and

$$\Delta_t \zeta = -\frac{g \Delta t m^2}{4 d^2 \bar{f}} JJ(E, \eta_e) \tag{20}$$

Next previously stored components of Vx are used to compute the advection by the divergent wind as follows:

$$\Delta_t \eta = -\frac{\Delta t m}{2d}\left[u_x(\eta_{i+1}^j - \eta_{i-1}^j) + v_x(\eta_i^{j+1} - \eta_i^{j-1})\right] \tag{21}$$

This result is added to (20) to produce fields of TADV.

Next these three advection schemes are compared using DADV as a basis and forming difference fields similar to those used for direct comparison of the winds.

Typical computer operating time including efficient handling of tapes and printing of output on an IBM 1402 printer is shown in Table I. Times shown are for one reporting period of one day at all levels.

Table I

Program	Run time in minutes
Solution of Balance Equation, (4)	46
Wind speed and directions from various inputs	18 (each)
Solution of equation (14) for χ	30
Solution of (16.a) and (16.b)	12
Comparison of winds	35
Advection of absolute vorticity with all winds	35
Comparison of advections	20
Preparation of grid field for FNWF plotter	4 (each)
Total	200 minutes.

It is apparent that operating time is a significant factor in restricting the amount of data collected.

4. Results

Results and conclusions are based on analyses of data selected from the period February 10 to 20, 1964. Only the United States is used in figures as it represents an area of reliable data. Using a small area for figures also allows display of finer detail. For illustration 0000Z 16 Feb 1964 was selected as it contains a wide range of synoptically interesting features over the United States.

Figure 1 depicts the pressure analysis (dashed lines) superimposed on the stream function analysis at 500 mb. The relative height difference at the semi-enclosed low center south of the Great Lakes is typical of the 500-mb level throughout the period studied. Figure 2 shows stream function analysis of the same period. Comparison with pressure height analysis indicates that the patterns are similarly related at other standard levels.

Wind speeds computed from 500-mb height and stream function analysis are shown in figure 4. Dashed isotachs enclose centers of maximum and minimum speeds. Speeds for other standard levels are shown in figures 2 and 3 where dashed lines are isotachs. Large numerals indicate values of minimum and maximum speeds. Analysis of speeds of these two winds shows there is a significant difference between them. Dashed lines in figure 5 (lower) are isolines of difference in wind speeds, geostrophic minus non-divergent. Similar analysis of other levels are shown in figures 6 and 7.

Figure 5 (upper) shows differences in direction for 500 mb, Dg - De. Solid lines show the 500-mb pressure height analysis, alternate dashed-dot lines are contours of negative 5-kt speeds, and dashed lines are 5-kt contours of positive difference. The area marked > 30 is almost completely within an area of wind speeds of less than 5 kt. Difference in directions are not shown for other levels but are easily located by reference to figures 2 and 3. Pillow and RMSD values for the hemispheric maps is given in figures 5 through 7. Note that P indicates that on the hemispheric scale Ve speed is lower at upper levels, e.g. by a factor of approximately 10 per cent at 300 mb. Except in regions of very sharp curvature or near singular points, DGDE, figure 5 (upper), is generally less than ten degrees at this and all other levels. A more detailed analysis was made of gridpoints and actual winds from 185 soundings in areas where DGDE was greater than 10 and both Ve and Vg exceed 5 kt. The graph in figure 8 shows the relationship found. It must be pointed out that interpolation within grid points was required to use actual soundings and that actual soundings are transmitted to the nearest 10 degrees only. In an effort to at least partially reduce effects of friction and local terrain effects the surface winds were not included in the data used for construction of this graph. "Va" is the actual wind as taken from the soundings and/or streamline analyses. A similar detailed analysis of speed differences was made using 210 soundings from areas where IGIE exceeded 10 knots. Results are shown in figure 9.

Maps of χ for 1000 mb (lower) and 300 mb (upper) are shown in figure 10. Dashed lines are 5 meter contours, solid lines are 2-kt intervals of wind speed, Ix. Figure 11 shows χ and Ix for 500 mb and 850 mb. These maps were plotted using an FNWF program designed for another purpose so that the contour labels have no intrinsic meaning. Contour interval is 10 meters. Note that the pre-trough region in low levels is associated with a χ maximum (point of Vx inflow) at upper levels and a χ minimum (point of Vx outflow) as would be reflected in divergence and convergence patterns associated with such height patterns.

Ix can be seen to be maximum at the 300-mb and 1000-mb levels. Note that these maximums are of the same magnitude, 8 to 10 knots, but that directions are opposite. As might be expected, speeds are minimum at 500 mb as a reflection of the minimum values of divergence known to exist there.

At 300 mb even maximum values represent a very small percent of the wind speed, seldom over 10 percent and generally less than three percent of Ve. With the lower wind speeds found at lower levels these same magnitudes of Ix are found in some instances to equal 45 percent of Ve. Such a case is depicted along the Gulf Coast in figure 8 (lower). It is of further interest that a deepening, fast-moving cold front was located in the same area almost directly under the 1000-mb Ix maximum center. This front moved rapidly up the East Coast and into the North Atlantic. A center of maximum Ix was associated with this front through-

out the traversal of the United States but speed of movement and the short period of accurate data prevented detailed study of this association.

Combining Ve and Vx, Vt was formed. Figure 12 (upper) shows the effects of this combination at 850 mb; 12 (lower) depicts 1000 mb. Solid lines are isotachs of Vt, dashed of Ve. The effect of this combination at middle and upper levels is so small as to be undetectable in this type analysis and is not shown. The effects at 1000 mb are quite evident. Detailed analysis of these proved that here there is a change in location of relative differences but no change in magnitude of the difference. Terrain and friction effects preclude any meaningful comparison of the small deviations from Ve to actual wind data. Further attempts to contrast Vt with Vg only further emphasizes that there is no significant difference between Vt and Ve.

Figures 12 and 13 depict the results of using Vg and Ve for advection of absolute vorticity. Solid lines are lines of zero advection using Vg, DADV; dashed lines are for Ve, EADV. The 300-mb level is omitted but showed no marked difference between the two advecting winds as it too showed practically congruent patterns. The numerals in the ratios shown are located at points of local minimum and maximum value, the upper numeral is for DADV. Units are 10^{-7} sec^{-1}. These values of change of vorticity are typical of the period investigated and showed DADV to be larger at both extremes by a factor of 5 to 10 units. Computing the pillow

and RMSD for all the standard levels gave a pillow O in every case and RMSD of 2 to 7 units with largest being at 300 mb. Use of Vt made no detectable difference in overall patterns. Some minor increases in value in the vicinity of sharp curvature at low levels was noted but were of the order of only 10 to 20 percent. Advection of vorticity with Vx was not computed as its significance has been seen to be small by its small effect when added to Ve. However, advection of temperature using Vx was computed using a program which evaluates the expressions

$$J(E,T) \tag{21}$$

and

$$V \cdot \nabla T \quad . \tag{22}$$

One hour change of temperature was computed. Figure 14 shows 1000-mb change of temperature with Ve (solid lines). Units are degrees celsius 10^{-1}. Detailed analysis of the grid map shows that advection with Vx over the entire map was less than $\pm$ 0.01 degrees over the United States except in the area along the Gulf Coast where values are depicted with a dashed contour enclosing an area of - 0.2 degrees. Here the advection with Vx actually exceeded EADV. This is the area noted earlier of the deepening low pressure system and front. Relatively large values were recorded at the 850-mb and 700-mb levels in this same area. Again the rapidity of movement of the front and associated values of advection and short length of the data period prevented detailed investigation but suggests the possibility of a meteorologically significant relationship.

5. Conclusions

1. Where there is curvature in the pressure patterns involved, the non-divergent velocity is a better approximation to the wind than the geostrophic value.

2. No significant change is made by combining the non-divergent and divergent winds for the uses investigated.

3. A relationship possibly exists between the divergent wind and frontal areas that could be utilized in locating such phenomena. This conclusion is based on very limited data but offers an interesting avenue for further investigation.

FIGURE 1

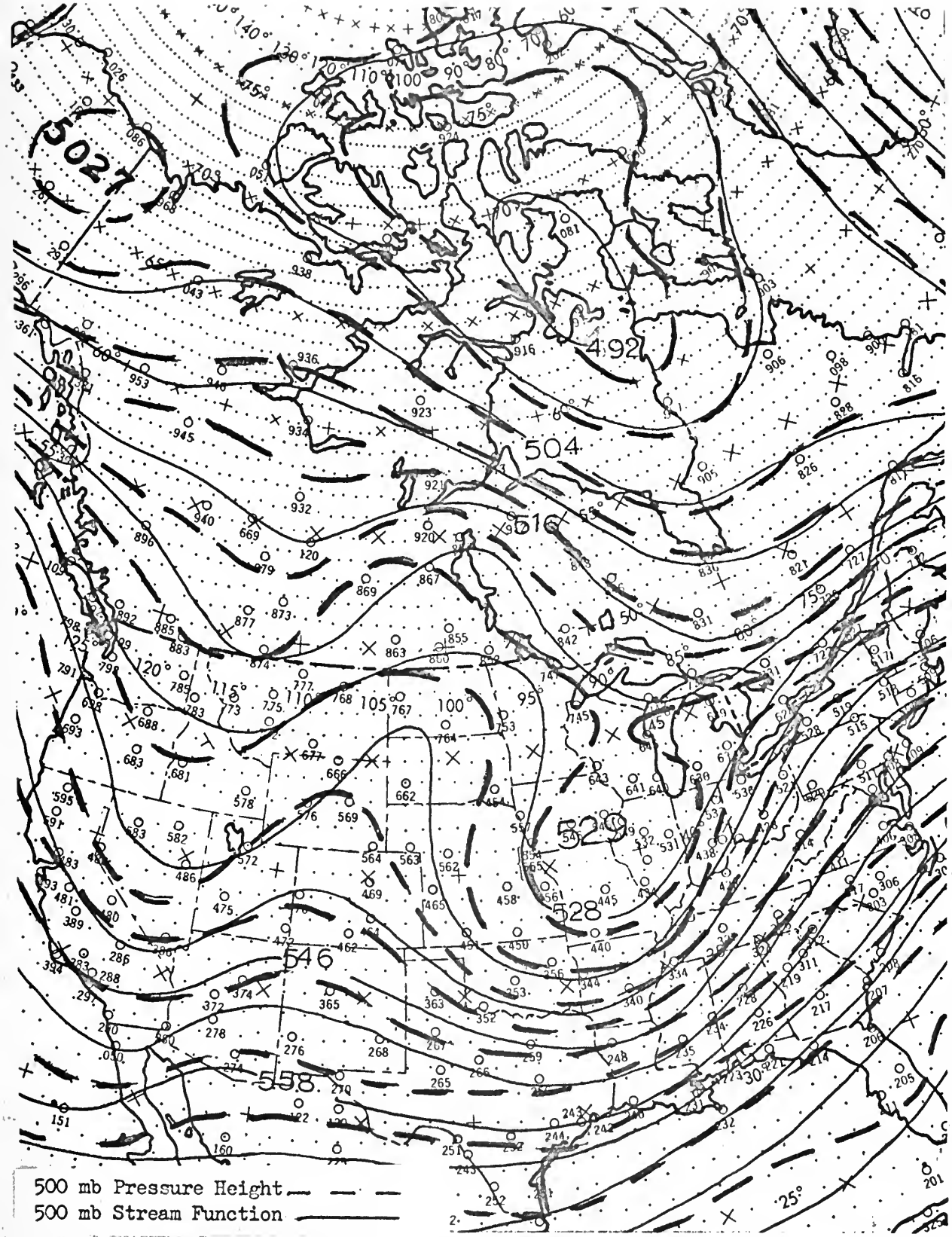

FIGURE 2

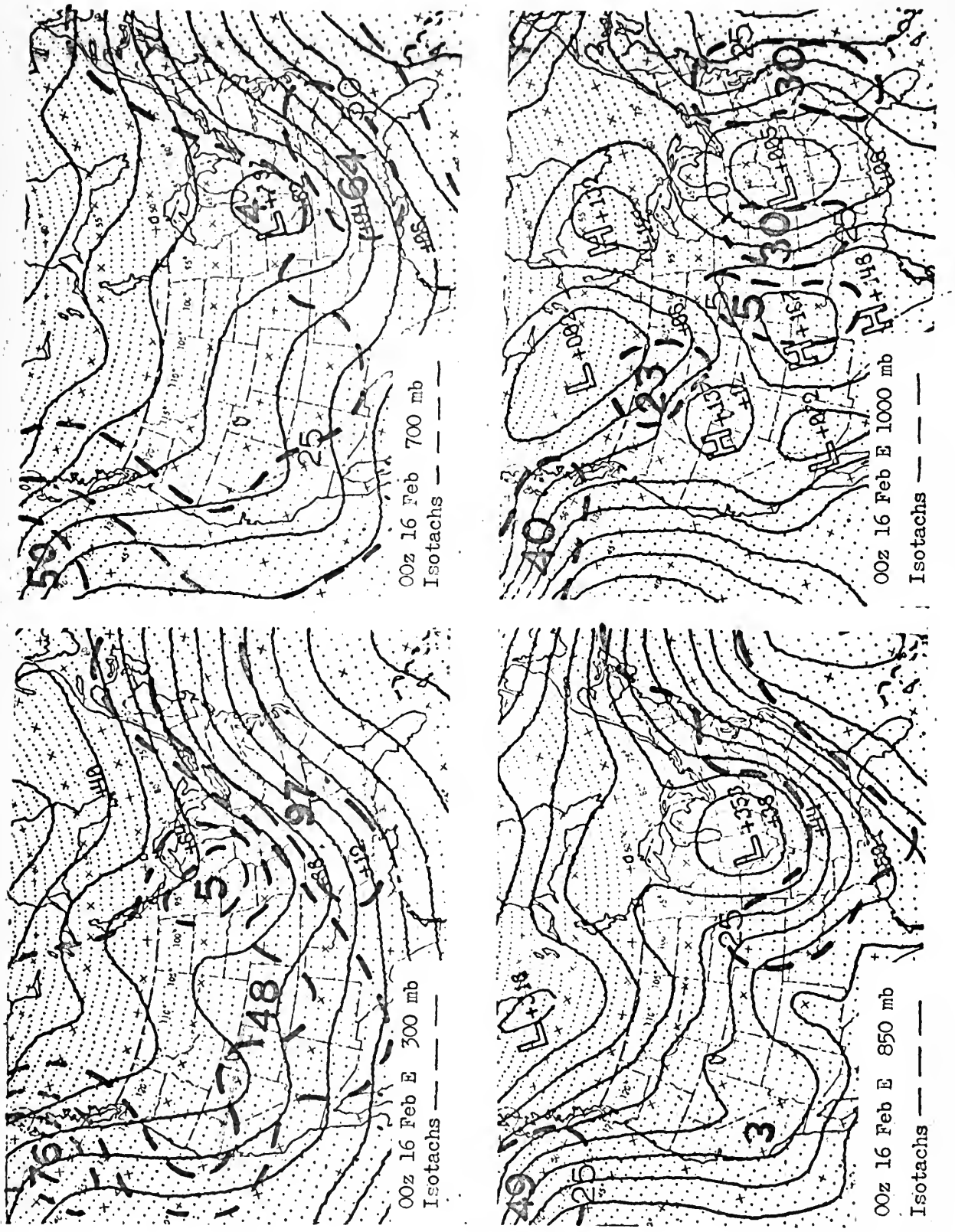
00z 16 Feb 700 mb
Isotachs
00z 16 Feb E 1000 mb
Isotachs
00z 16 Feb E 300 mb
Isotachs
00z 16 Feb E 850 mb
Isotachs

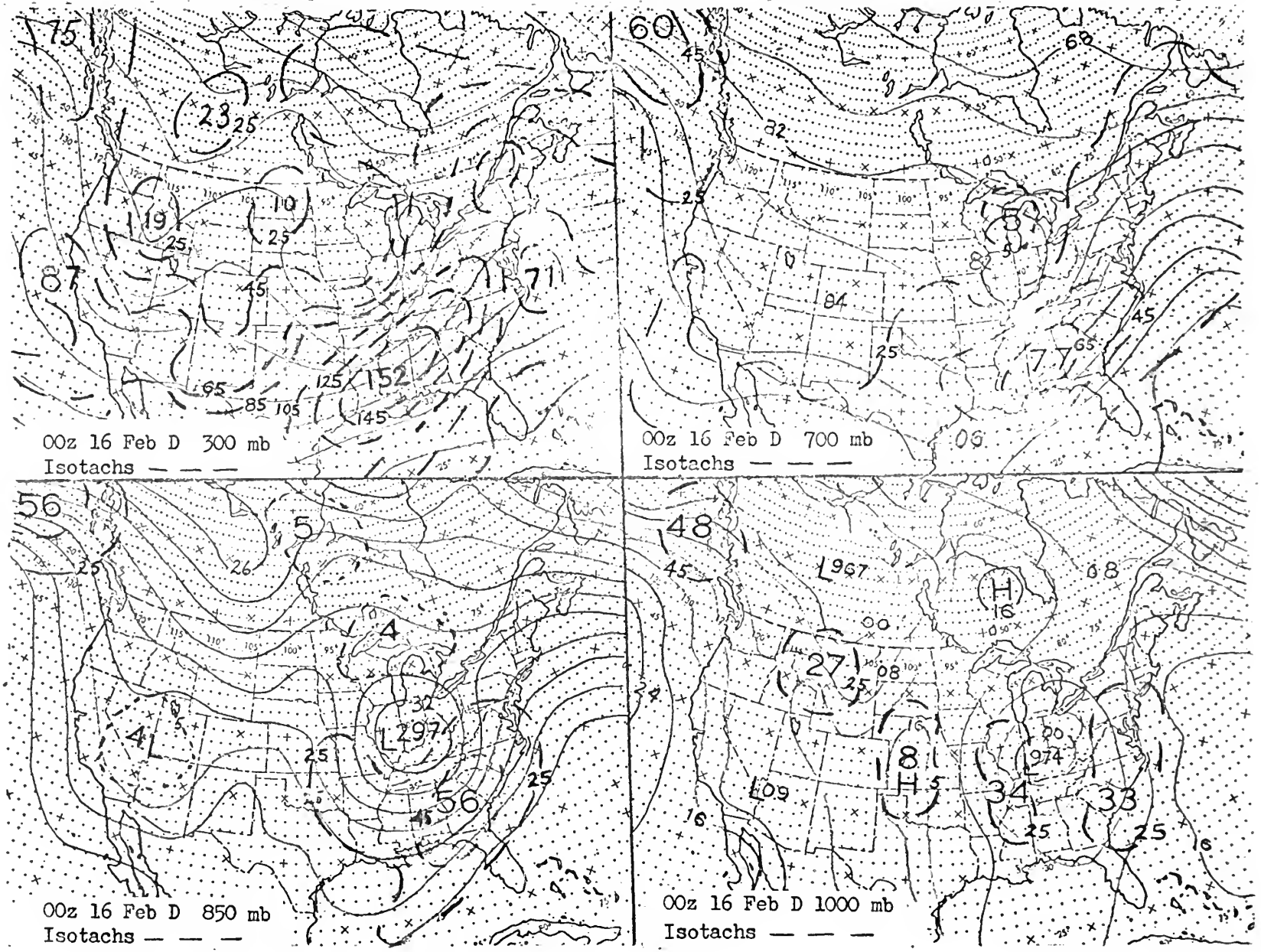
00z 16 Feb D 300 mb
Isotachs — — —
00z 16 Feb D 700 mb
Isotachs — — —
00z 16 Feb D 850 mb
Isotachs — — —
00z 16 Feb D 1000 mb
Isotachs — — —

FIGURE 3

FIGURE 4

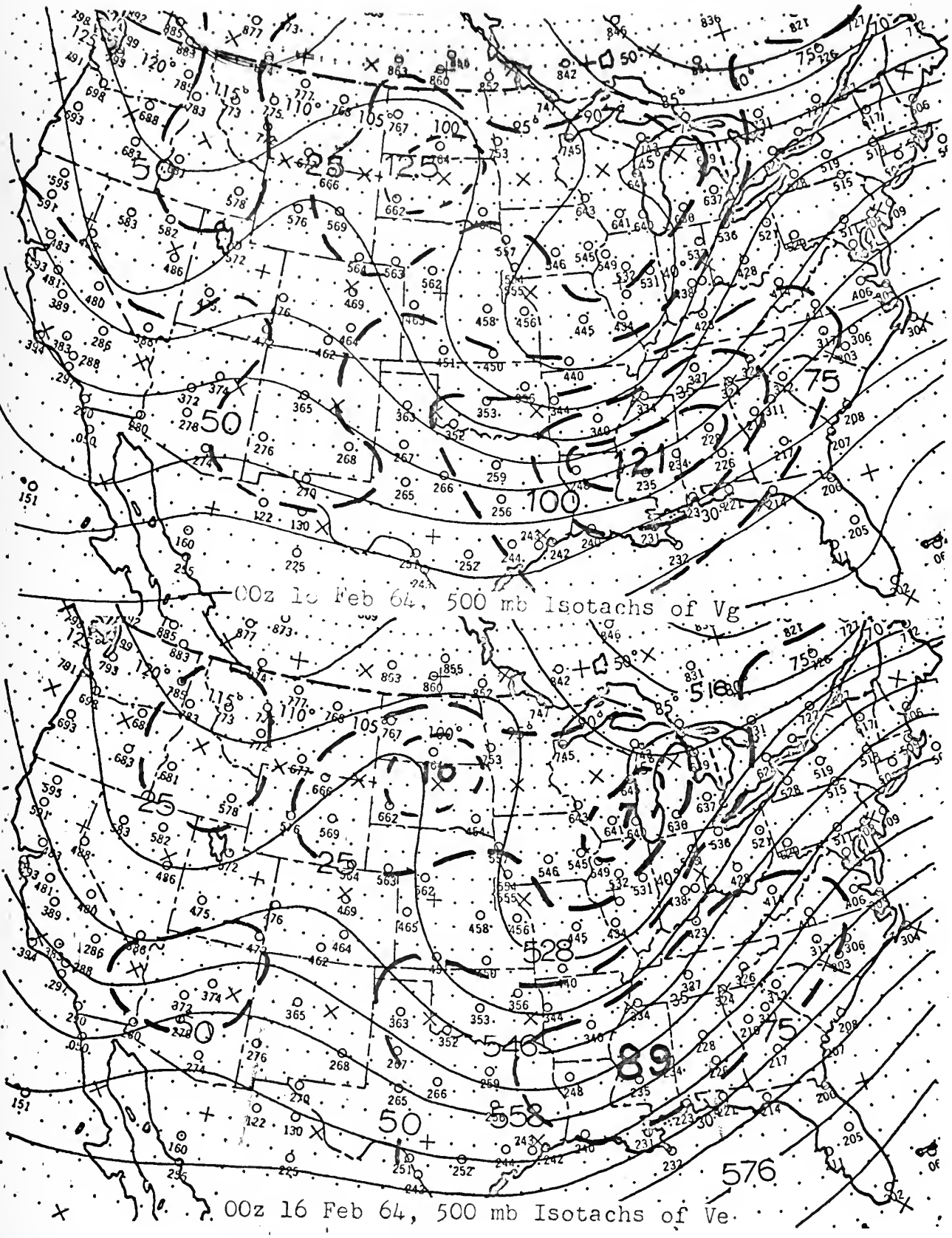
00z 16 Feb 64, 500 mb Isotachs of Vg
00z 16 Feb 64, 500 mb Isotachs of Ve

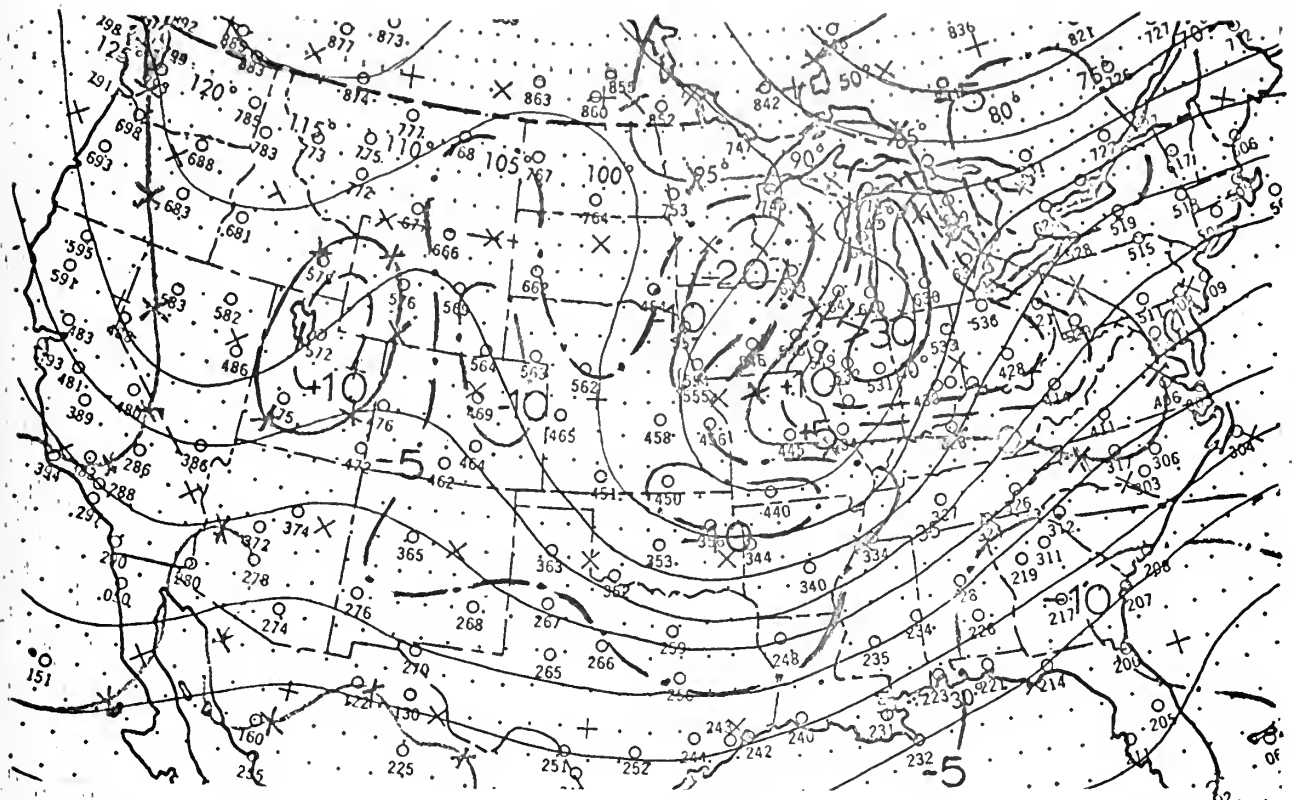

00z 16 Feb Difference in wind directions, Geostrophic - Non-divergent; 500 mb

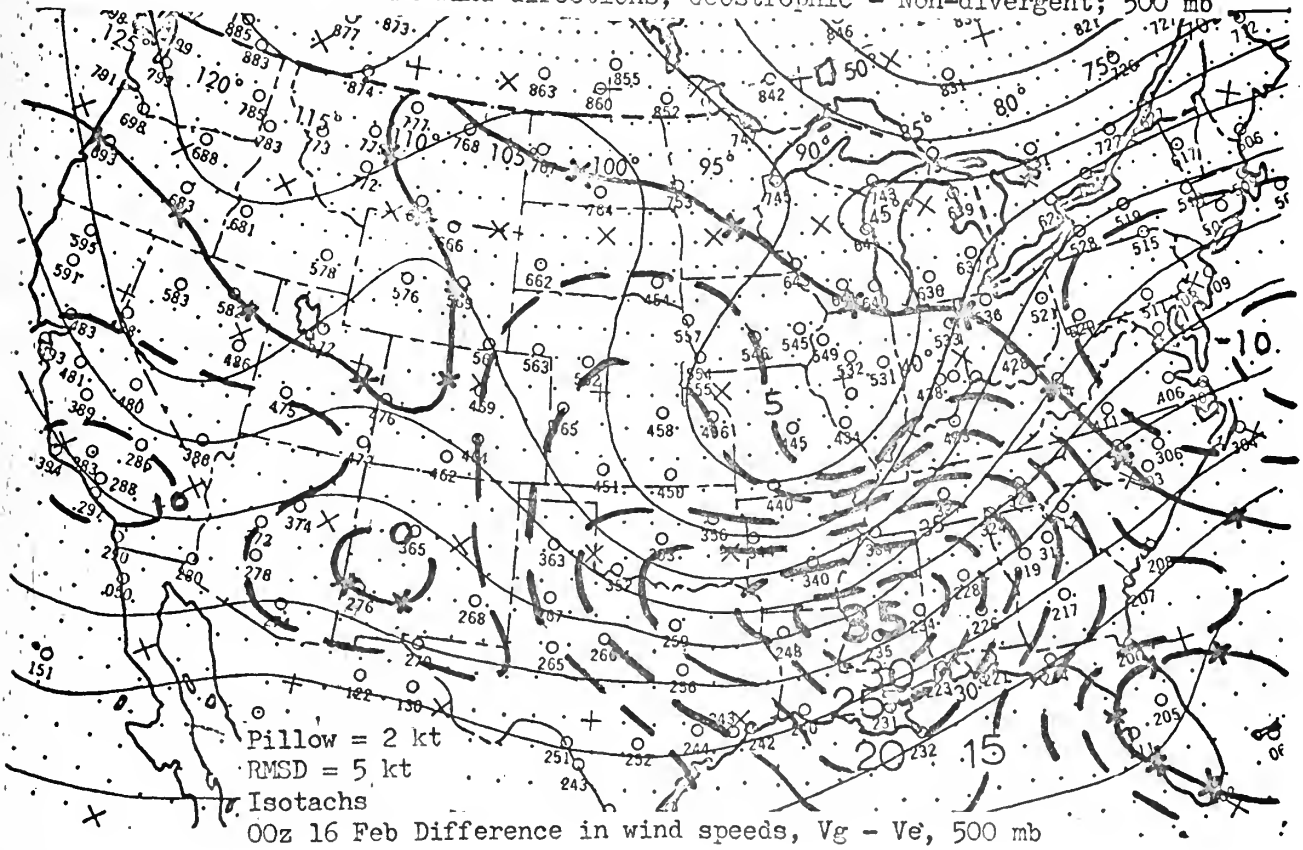

00z 16 Feb Difference in wind speeds, Vg - Ve, 500 mb

FIGURE 6

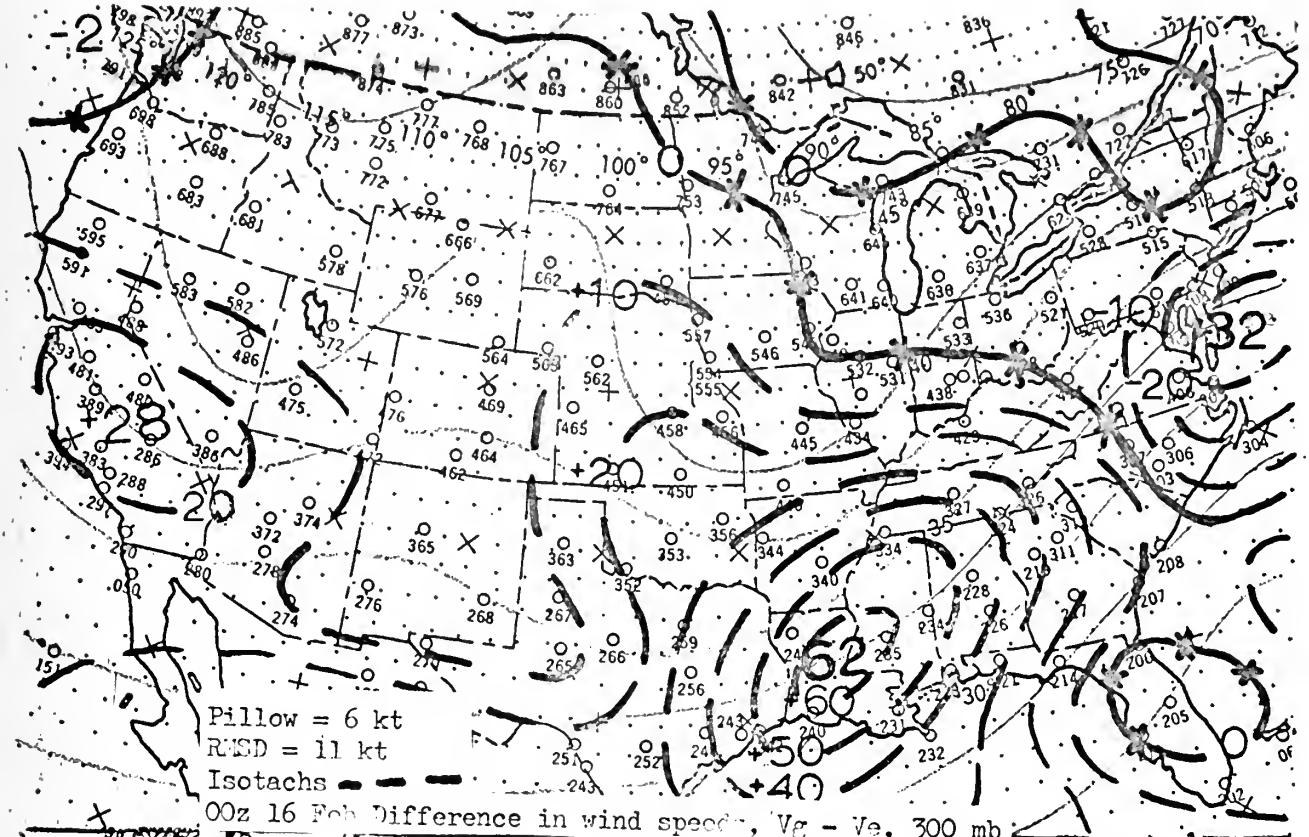

00z 16 Feb Difference in wind speeds, Vg - Ve, 300 mb

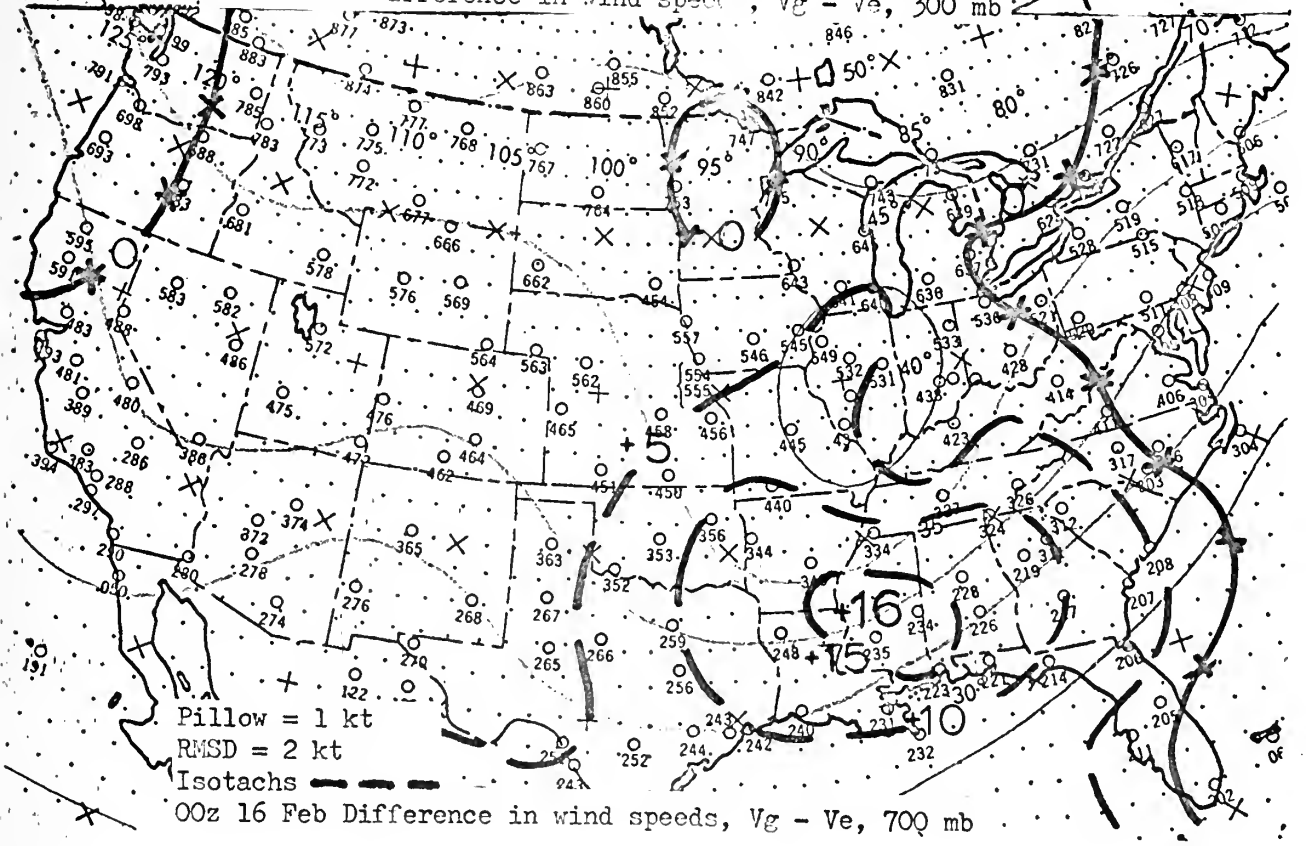

00z 16 Feb Difference in wind speeds, Vg - Ve, 700 mb

FIGURE

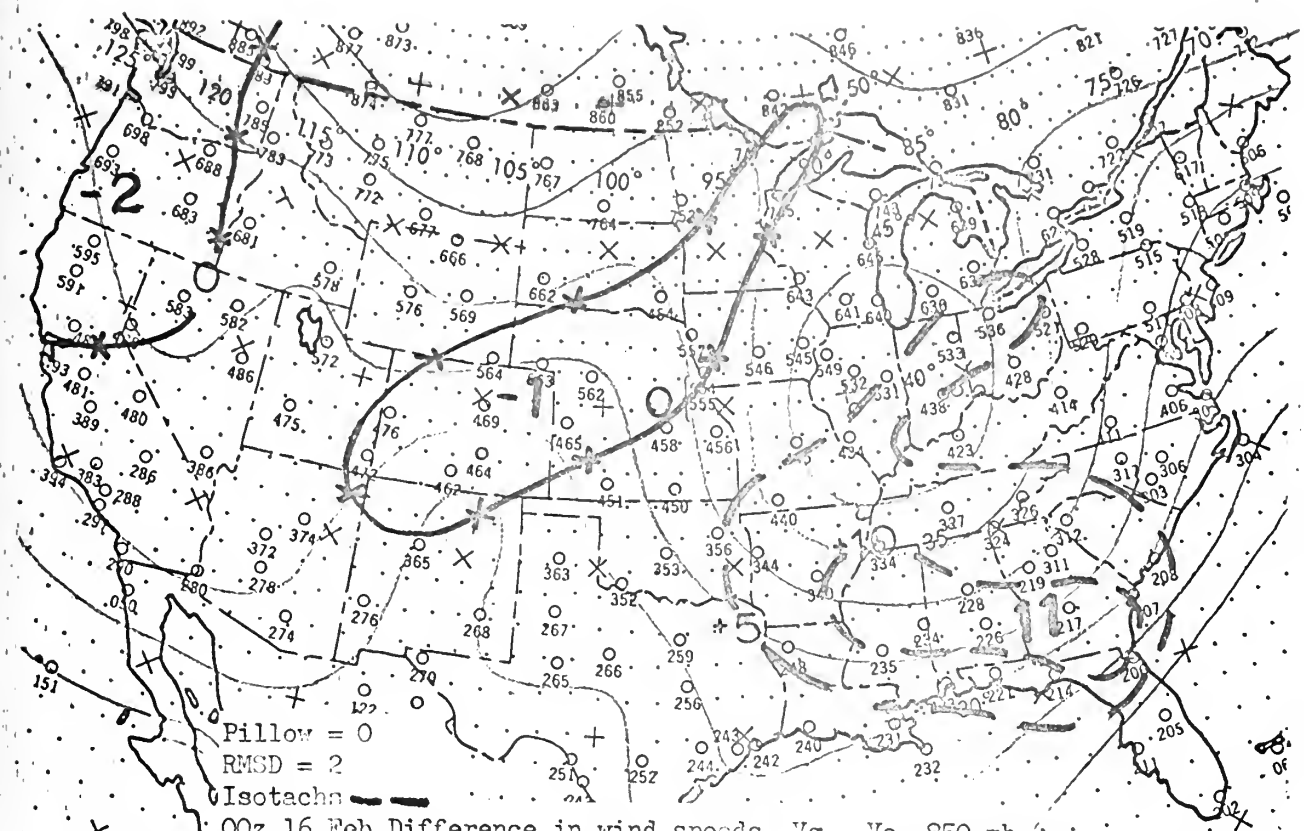

00z 16 Feb Difference in wind speeds, Vg - Ve, 850 mb

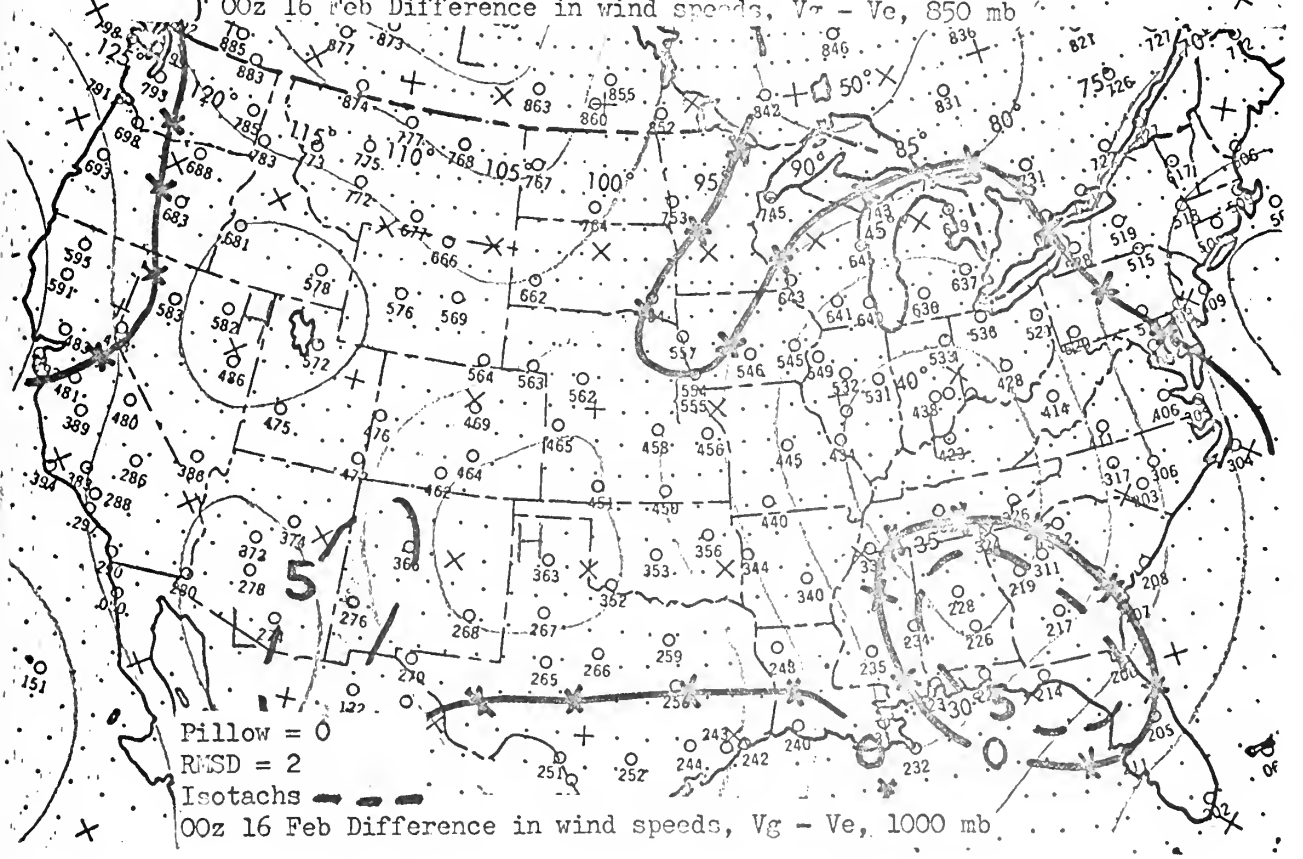

00z 16 Feb Difference in wind speeds, Vg - Ve, 1000 mb

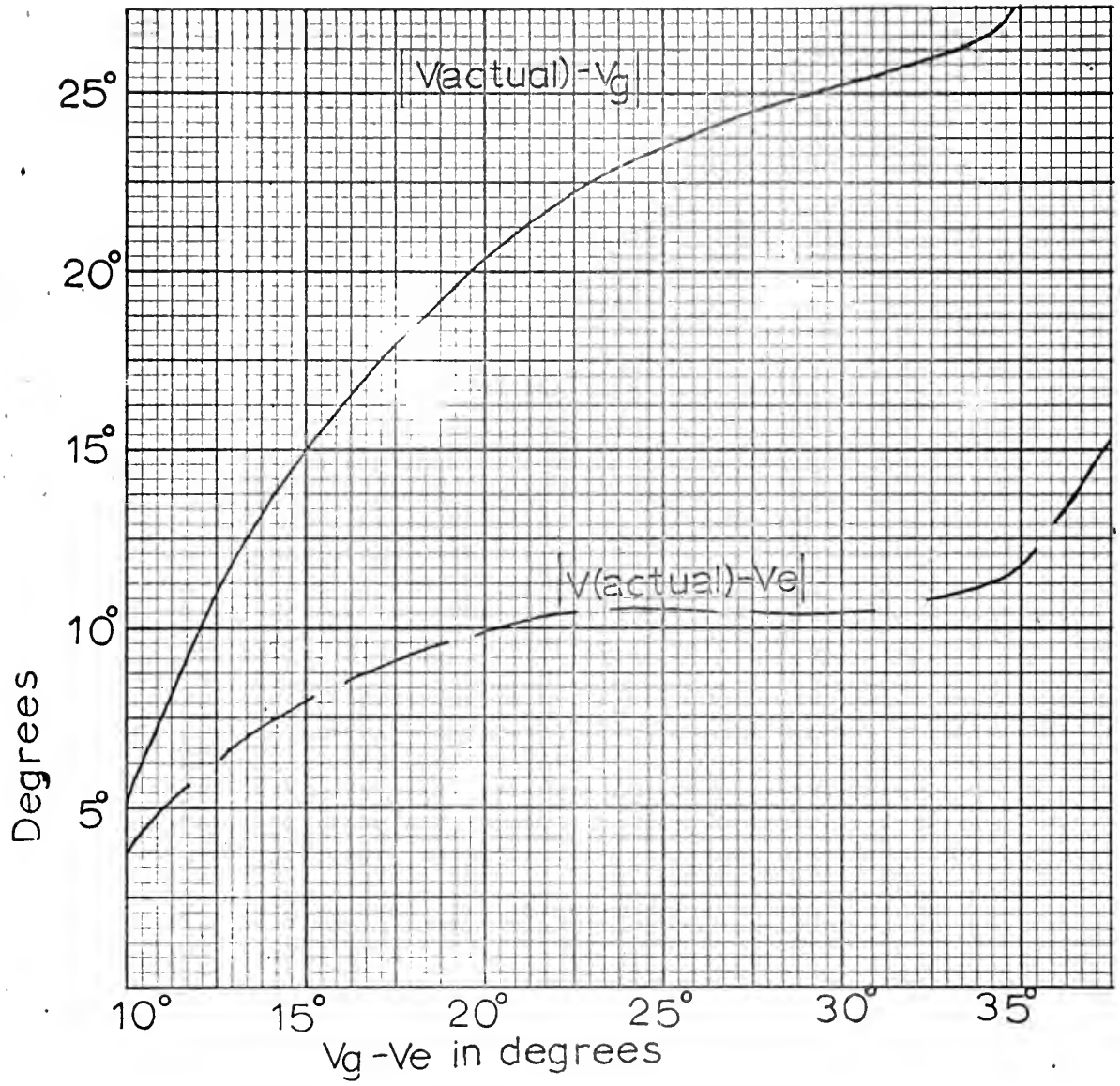
|V(actual)-Vg|
|V(actual)-Ve|
25°
20°
15°
10°
5°
Degrees
10°
15°
20°
25°
30°
35°
Vg -Ve in degrees

FIGURE 9

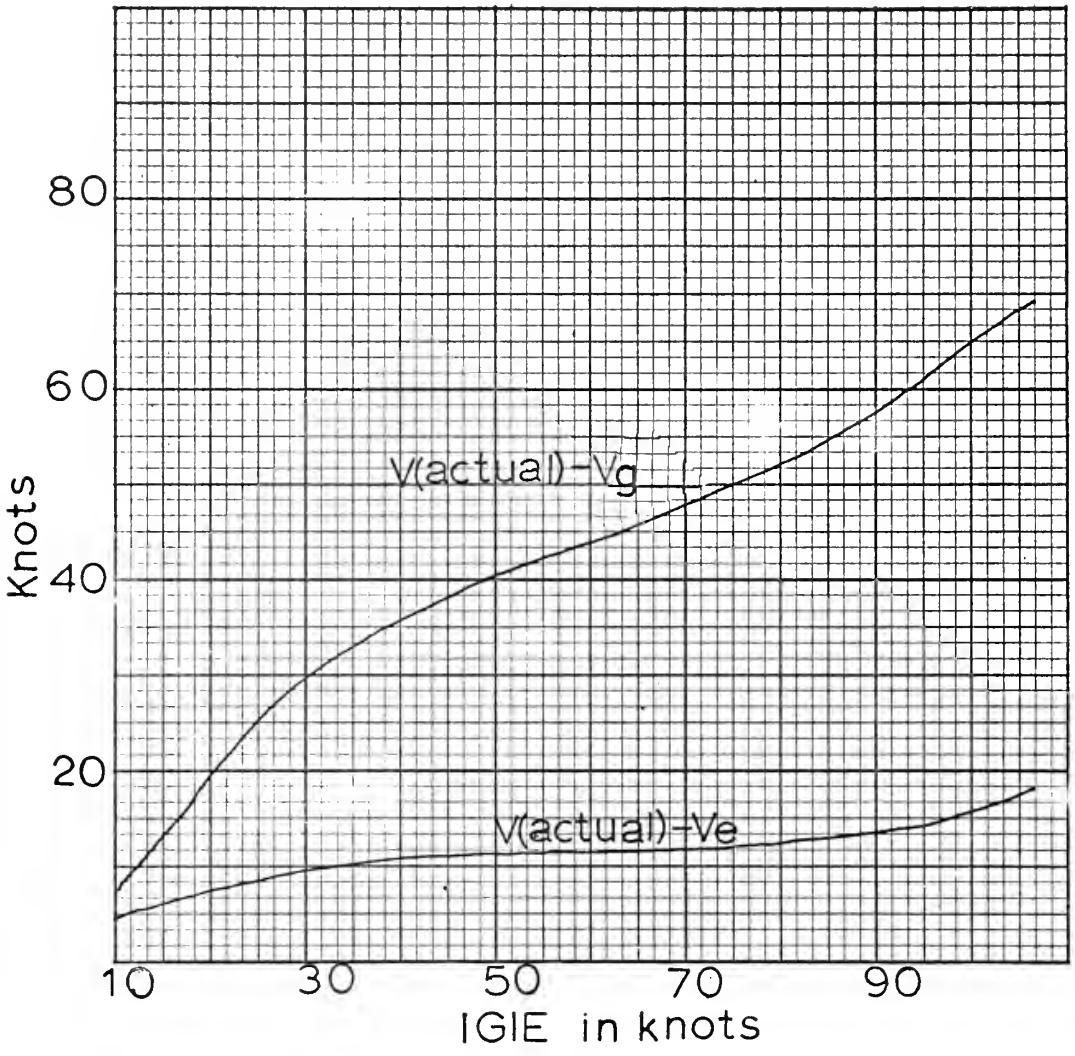
80
60
40
20
Knots
V(actual)-Vg
V(actual)-Ve
10
30
50
70
90
IGIE in knots

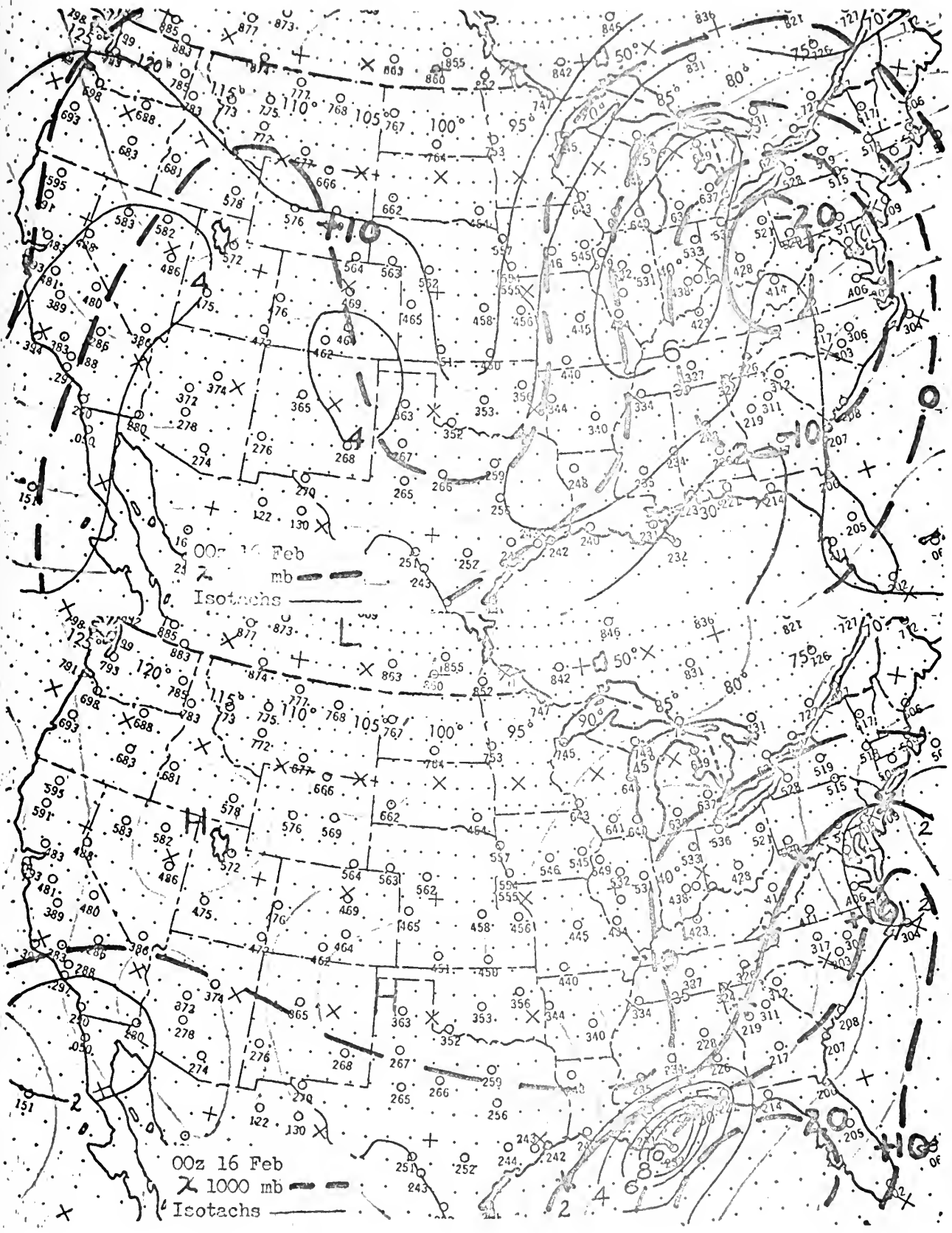
00z 16 Feb
1000 mb
Isotachs
00z 16 Feb
1000 mb
Isotachs

FIGURE 11

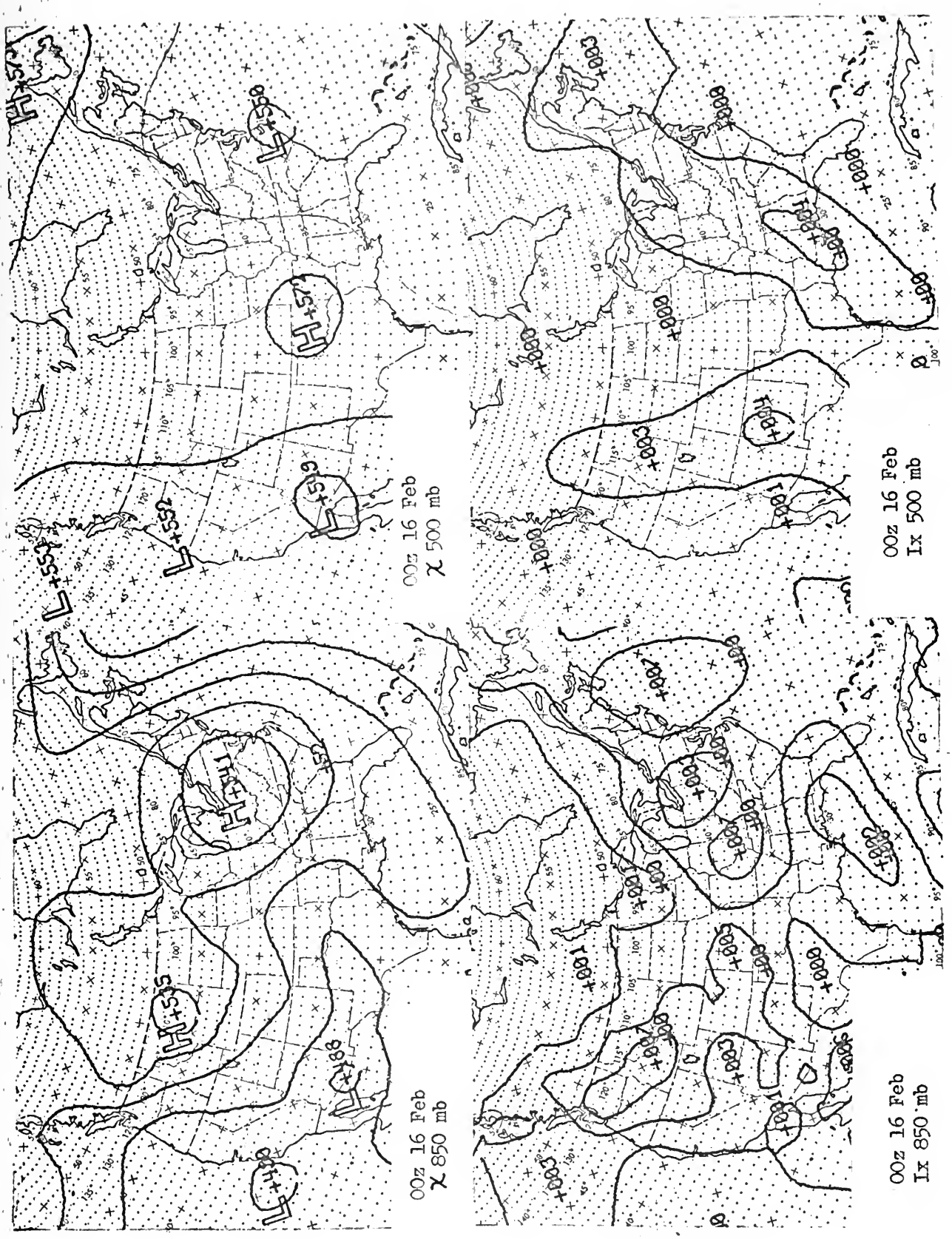
00z 16 Feb
χ 500 mb
00z 16 Feb
Ix 500 mb
00z 16 Feb
χ 850 mb
00z 16 Feb
Ix 850 mb

FIGURE 12

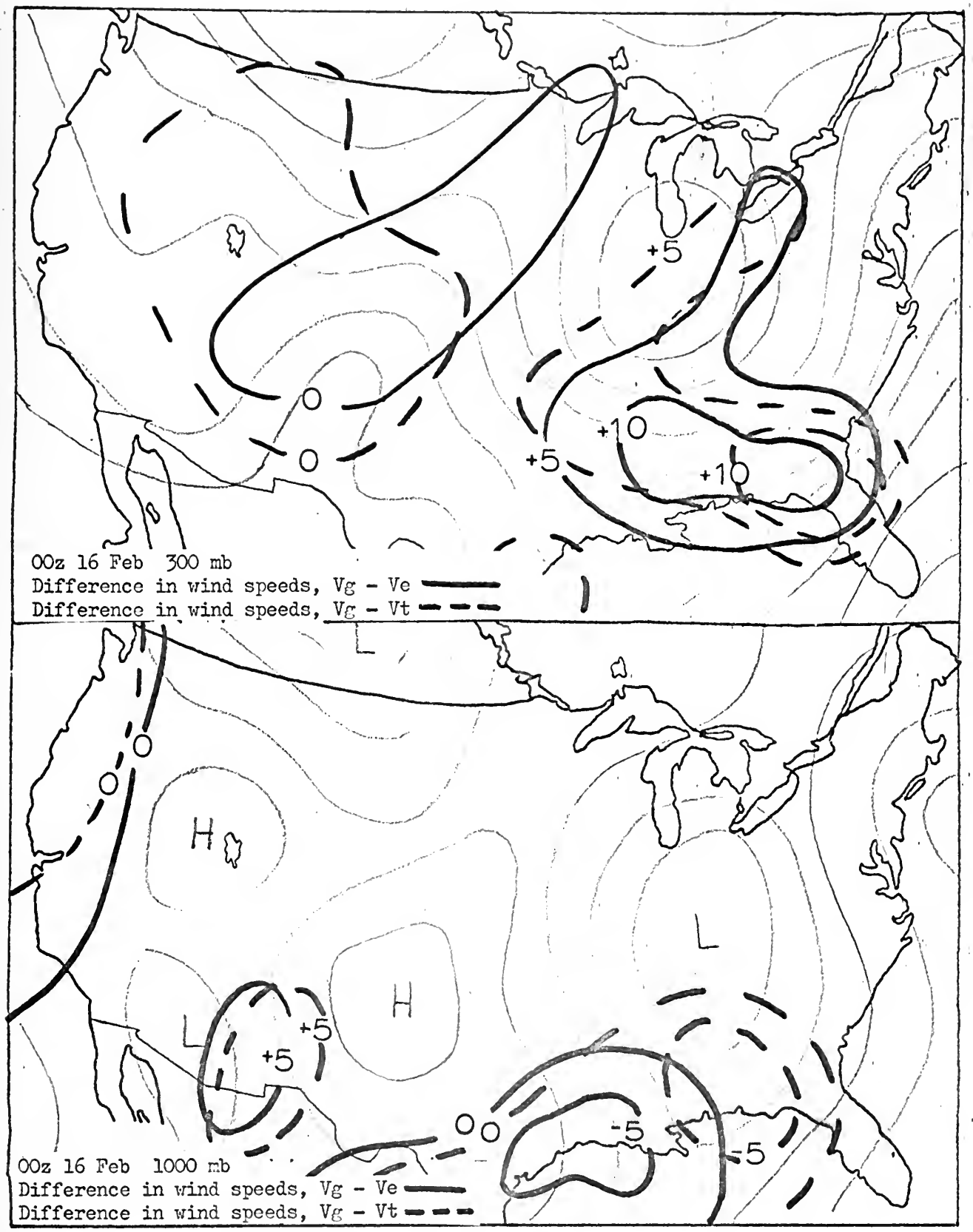
+5
0
0
+10
+5
+10
00z 16 Feb 300 mb
Difference in wind speeds, Vg - Ve
Difference in wind speeds, Vg - Vt
L
0
0
H
H
L
L
+5
+5
0
0
-5
-5
00z 16 Feb 1000 mb
Difference in wind speeds, Vg - Ve
Difference in wind speeds, Vg - Vt

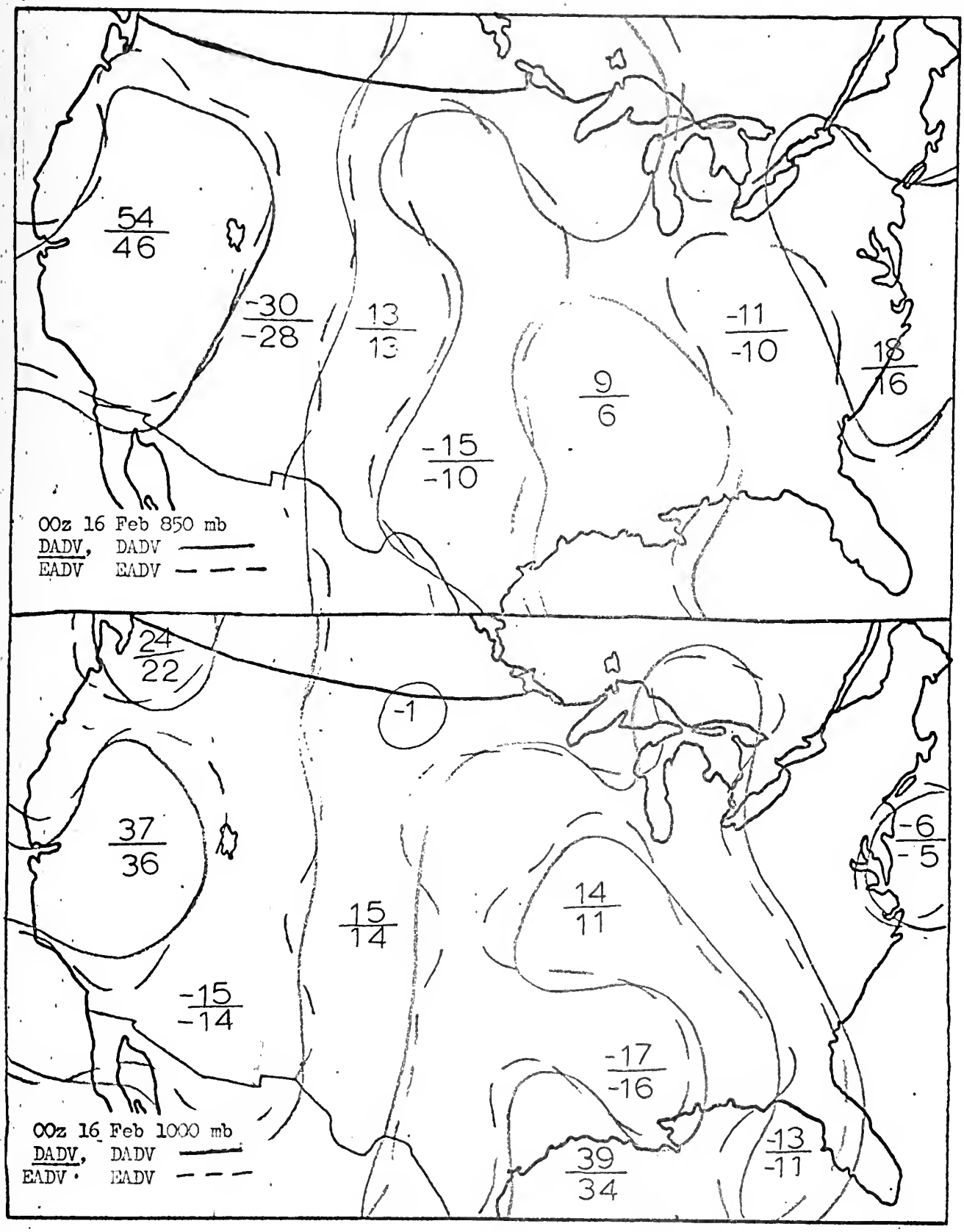
54
46
-30
-28
13
13
-11
-10
18
16
9
6
-15
-10
00z 16 Feb 850 mb
DADV, DADV
EADV EADV
24
22
-1
37
36
15
14
14
11
-6
-5
-15
-14
-17
-16
-13
-11
39
34
00z 16 Feb 1000 mb
DADV, DADV
EADV EADV

FIGURE 14

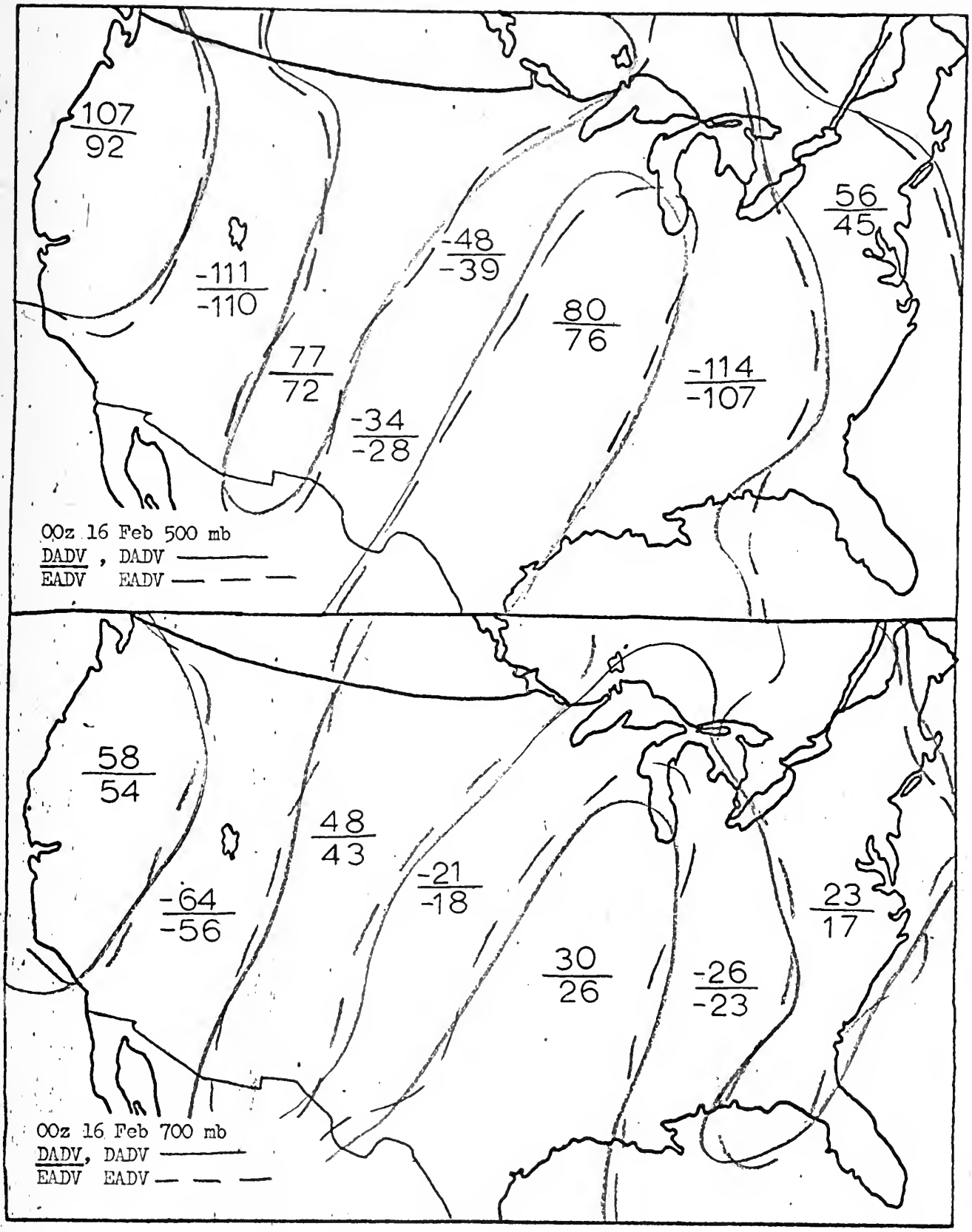
107
92
-111
-110
77
72
-34
-28
-48
-39
80
76
-114
-107
56
45
00z 16 Feb 500 mb
DADV , DADV
EADV EADV
58
54
-64
-56
48
43
-21
-18
30
26
-26
-23
23
17
00z 16 Feb 700 mb
DADV, DADV
EADV EADV

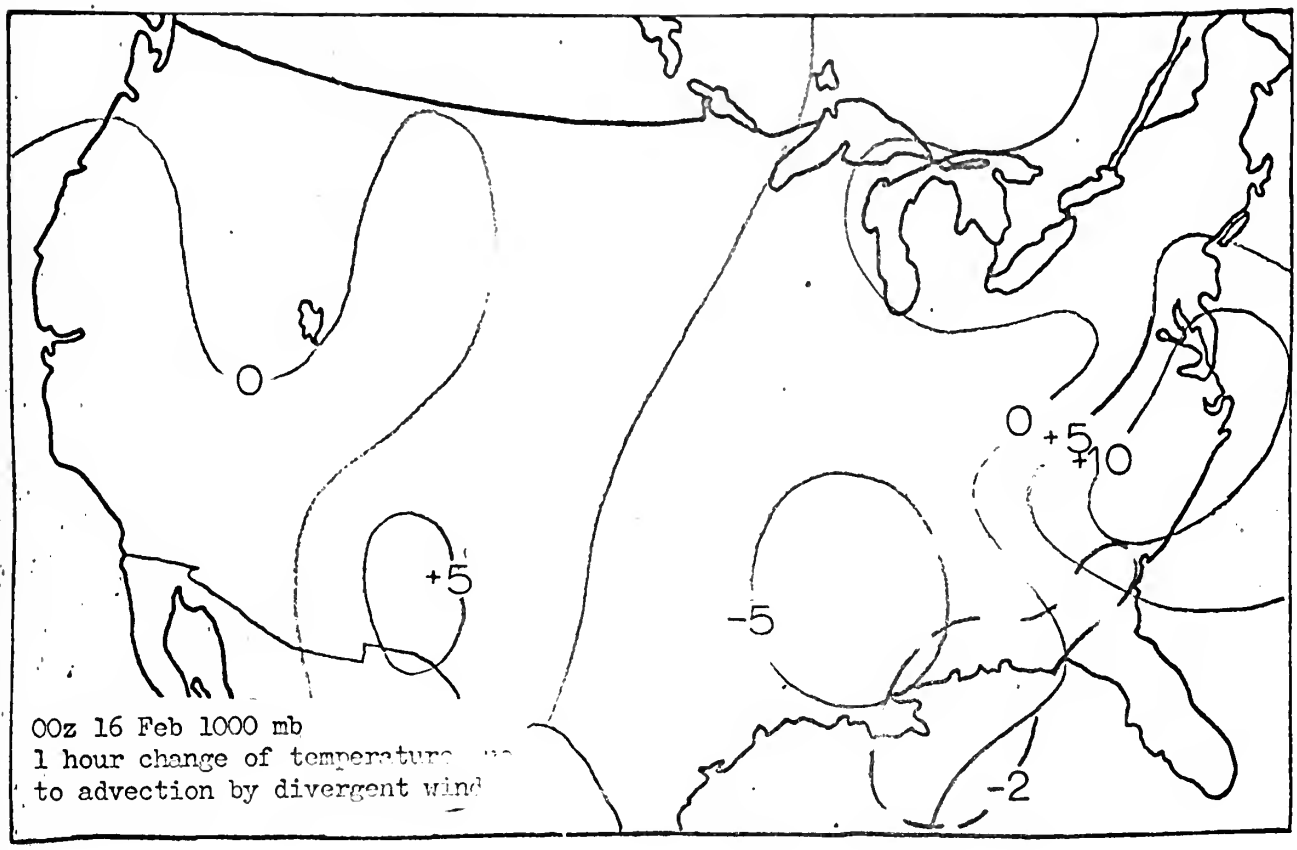

00z 16 Feb 1000 mb
1 hour change of temperature [illegible]
to advection by divergent wind

BIBLIOGRAPHY

1. Haltiner, G. J., L. C. Clarke, and G. E. Lawniczak, Computation of Large Scale Vertical Velocity, J. of App. Meteor., vol. 2, No. 2 April 1963, pp. 242-259.

2. Alden, R. F., and G. C. Rosenberger, Distribution of tropospheric velocity divergence with respect to pressure systems, M. S. Thesis, U. S. Naval Postgraduate School, Monterey, California.

APPENDIX I

Pillow is defined as

$$P = \frac{\sum_{n=1}^{X=n=3968} (A-B)_n}{X} \quad . \tag{I-1}$$

The root-mean-square differnece (RMSD) is determined as follows:

$$RMSD = \sqrt{\sum_{n=1}^{X=n=3968} \left[(A-B)-P\right]_n^2 / X} \quad . \tag{I-2}$$

In equations (I-1) and (I-2), A_n and B_n represent the point values of the fields being compared. In this example the A value is a geostrophic value of speed or direction and B is the corresponding value of either non-divergent or total wind.